Nuclear Instruments and Methods in Physics Research B 303 (2013) 22–26

Contents lists available at SciVerse ScienceDirect

Nuclear Instruments and Methods in Physics Research B

journal homepage: www.elsevier.com/locate/nimb

Molecular dynamics study of polystyrene bond-breaking and crosslinking under C_{60} and Ar_n cluster bombardment

Bartlomiej Czerwinski [a,*], Zbigniew Postawa [b], Barbara J. Garrison [c], Arnaud Delcorte [a]

[a] Institute of Condensed Matter and Nanosciences – Bio & Soft Matter (IMCN/BSMA), Université Catholique de Louvain, 1 Croix du Sud, B-1348 Louvain-la-Neuve, Belgium
[b] Smoluchowski Institute of Physics, Jagiellonian University, ul. Reymonta 4, 30-059 Krakow, Poland
[c] Department of Chemistry, The Pennsylvania State University, University Park, PA 16802, USA

ARTICLE INFO

Article history:
Received 19 July 2012
Received in revised form 31 October 2012
Accepted 1 November 2012
Available online 29 December 2012

Keywords:
Molecular dynamics
Cluster SIMS
Molecular depth profiling
Crosslinking
Desorption
Polystyrene

ABSTRACT

Molecular dynamics computer simulations are used to elucidate the bond-breaking and crosslinking processes induced by 2.5 keV C_{60} and Ar_n cluster bombardment in an amorphous sec-butyl-terminated polystyrene sample. The obtained results indicate that replacement of C_{60} by Ar_{18} or Ar_{60} projectiles leads to the decrease of the number of broken bonds and, hence, to the decrease of formation of new intra- and intermolecular (crosslinking) bonds. When the number of atoms in the Ar_n cluster is increased from 60 to 250 or more, the total number of broken bonds and the total number of newly created bonds reach a zero value. Additional comparison to the case of a fullerite crystal reveals that the change of material properties leads to almost 7.5-fold reduction of the efficiency of the crosslinking process.

1. Introduction

Over the last few decades energetic ion beams have become important processing and characterization tools for a broad segment of the scientific and technological manufacturing sector. Nowadays, atoms, molecules and atomic and molecular clusters are routinely used for surface analysis and treatment through the use of techniques like secondary ion mass spectrometry (SIMS) [1,2], desorption electrospray ionization (DESI) [3–5] mass spectrometry or the recently developed desorption ionization by charge exchange (DICE) [6,7]. The main application fields are in microelectronics, nanotechnology and biological research.

The introduction of cluster ion guns such as SF_5, C_{60}, Au_n, Bi_n and Ar_n resulted in a particular acceleration of the development of the SIMS technique. Their implementation allows for new protocols for the analysis of sensitive organic materials and, especially, biological samples [1]. The latest research reveals that large clusters composed of thousands of argon atoms produced by supersonic expansion of high-pressure gas through a nozzle with an energy of a few eV per atom (originally developed for surface smoothing [8]) are able to produce relatively high yields of molecular ions with low (and tunable) fragmentation [9]. Unlike SF_5 and C_{60}, the Ar_n clusters are capable of depth profiling most types of organic materials used so far for analysis [2,10].

Energetic cluster ion bombardment of organic materials initiates processes which lead to many chemical reactions within the bombarded samples. The main issues observed for polymers during depth profiling experiments, is thought to be the formation of crosslinks within the bombarded sample and/or the graphitization of its surface [2]. In general the crosslinking process is understood as the formation of new bonds between different molecules or polymeric chains which usually leads to the formation of large chunks of newly bonded material and to the significant reduction of sputtering efficiency. On the other hand, the carbonization of the surface, is the formation of a carbon layer on the surface of the bombarded material. This process is usually the consequence of the fragmentation of the organic material initiated by impinging projectiles, leading to the creation of a large number of free, highly reactive, carbon radicals which may combine to form a compact, usually amorphous, structure. With continuous bombardment, this compact structure can significantly increase its volume and, as a consequence, begin to block the emission of organic material located below [2].

In this research, classical molecular dynamics (MD) computer simulations are used as a tool for the theoretical insight into the bond-breaking and the new bond formation processes in an amorphous sec-butyl-terminated polystyrene sample, initiated by the irradiation with C_{60} and Ar_n (n = 18, 60, 250, 500, 1000, 1700,

* Corresponding author. Tel.: +32 10478460; fax: +32 10473452.
E-mail address: bartlomiej.czerwinski@uclouvain.be (B. Czerwinski).

0168-583X/$ - see front matter © 2013 Elsevier B.V. All rights reserved.
http://dx.doi.org/10.1016/j.nimb.2012.11.030

2500) clusters with the initial total kinetic energy of 2.5 keV. The number of broken bonds as well as the number of newly created internal and external bonds are analyzed for each projectile bombardment. The formation of new intermolecular bonds at each impact can be regarded as the premise of the crosslinking process which, in the experiments, is observed as the result of continuous ion bombardment of the sample. In this study, we focus on the analysis of a single cluster bombardment event to compare different cluster projectiles and to provide predictions for their use in the real world situations.

2. Model

The detailed description of the computer simulation method used to model cluster bombardment can be found elsewhere [11]. Briefly, the motion of the particles is determined by integrating Hamilton's equations of motion. The forces among the particles are described by a blend of pairwise additive and many-body potential energy functions. The Ar–C and Ar–H interactions are described using the purely repulsive pairwise KrC potential [12]. To calculate the interactions between Ar atoms, a Lennard-Jones potential is used [13]. It is splined with the KrC potential at low interatomic distances to properly describe high-energy collisions [12]. The many-body adaptive intermolecular potential, AIREBO, developed by Stuart and co-workers is used for H–H, H–C and C–C interactions [14]. This potential is based on the reactive empirical bond order (REBO) potential developed by Brenner for hydrocarbon molecules [15]. The model approximating the amorphous sec-butyl-terminated polystyrene (aPS4) surface consists of 24,500 PS4 molecules (1,911,000 atoms) [16]. The size of the sample is approximately 317.3×317.2 Å^2 in surface area and 236.2 Å in depth. The sample is surrounded by a zone of rigid atoms and a Langevin heat bath region with a thickness of 20 and 30 Å, respectively, to prevent pressure waves generated by the cluster projectile impact from reflecting off the system boundaries and to keep the sample at the required temperature of 0 K [17]. The aPS4 sample is bombarded by C_{60} and Ar_n (n = 18, 60, 250, 500, 1000, 1700, 2500) cluster projectiles which are directed normal to the surface. All simulations are stopped after 3 ps. To calculate the number of broken bonds and newly created internal and external bonds at each chosen time step (Δt = 100 fs) of analysis, the list of atoms bonded to each atom in the system is checked and compared to the list of atoms bonded to the same atom in its initial state (t = 0 fs). Since the analysis is done based on the "snapshots" of the entire system taken from the MD simulations at the predefined time steps, the atoms bonded to each individual atom within the bombarded system are searched based on atoms relative distance. The threshold value for this distance (maximum search radius) is taken at the half of the potential well of interaction between atoms in the equilibrium state, as defined by the attractive part of the AIREBO potential [14]. This gives 1.27, 1.495 and 1.79 Å for H–H, H–C and C–C interactions, respectively. When the list of atoms bonded to the each individual atom is changed it is classified as (1) creating a new external bond, if it has a new bonded atom initially originating from the different molecule, as (2) creating a new internal bond, if it has a new bonded atom initially originating from the same molecule or (3) broken, if the number of bonded atoms is reduced but it does not create any new external or internal bonds. The atom is classified as (4) intact, if its bonded atom list does not change. Additionally, molecules containing different types of atoms are marked according to the same rules, as containing new external bonds, containing new internal bonds, broken or intact. The reader should note that, since, in general, the algorithm used for the calculation of broken and newly created bonds takes into account all H–H, H–C and C–C interactions, not all newly created external bonds can be considered as crosslinks. To properly calculate the number of newly created crosslinks, the additional analysis is performed, in which only intermolecular C–C interactions are taken into account. This is done in agreement with the experimental point of view, in which the crosslinking bond in polystyrene sample is considered as a new bond created between two carbon atoms belonging to two different PS molecules.

3. Results and discussion

The cross-sectional view of the aPS4 sample bombarded by C_{60} and Ar_n cluster projectiles, at 3 ps after the impact, is shown in Fig. 1. The craters which are formed during C_{60} and small argon cluster (n < 250) bombardment have similar diameters and depths. This indicates that the physics of the sputtering process initiated in the aPS4 sample by these projectiles is very similar, which is in good agreement with the results obtained for benzene [18]. With increasing size of the Ar cluster, the lateral size of the forming crater increases, while its depth decreases. This is an effect of the de-

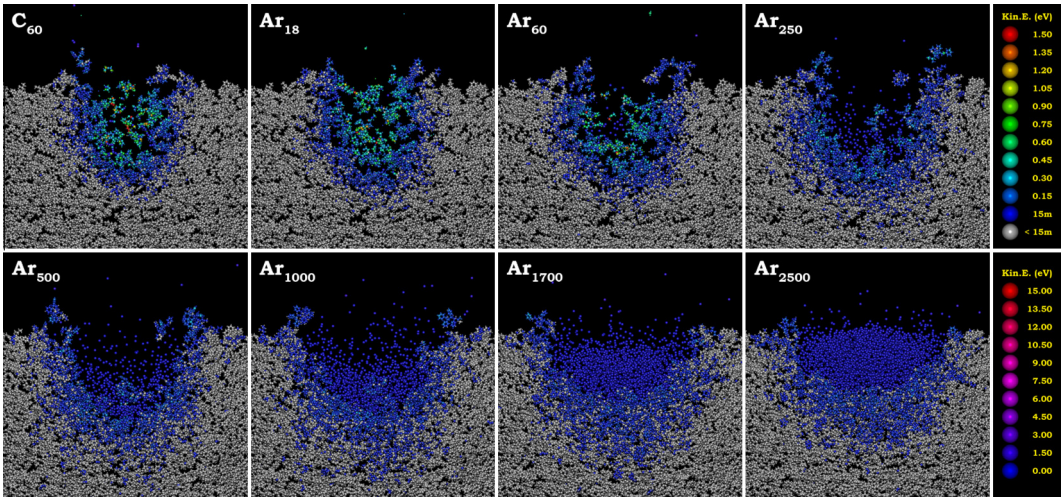

Fig. 1. The zoomed side cross-sectional view of the sample at 3 ps after bombardment by C_{60} and Ar_n (n = 18, 60, 250, 500, 1000, 1700, 2500) clusters. The colors represent the kinetic energy of atoms. The color coding for polystyrene and projectile atoms is shown in the top and bottom color bar, respectively. (For interpretation of the references to colour in this figure legend, the reader is referred to the web version of this article.)

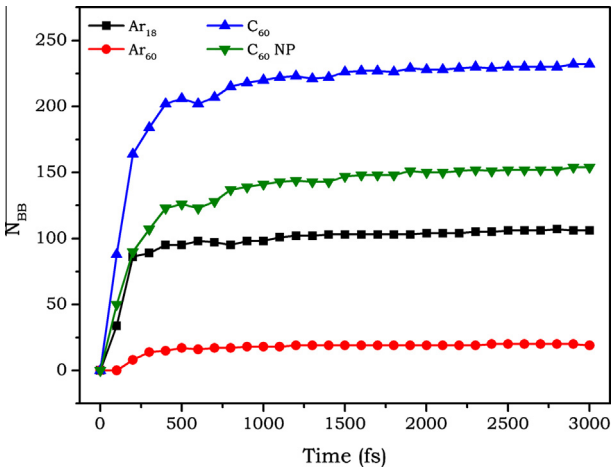

Fig. 2. The time evolution of number of bonds broken during 2.5 keV cluster bombardment of amorphous polystyrene sample. Since there is no bond-breaking for Ar_n clusters with $n \geqslant 250$, only Ar_{18}, Ar_{60} and C_{60} are shown. The C_{60} NP signature represents the analysis of the C_{60} bombardment in which bonds broken within projectile are not taken into account. (For interpretation of the references to colour in this figure legend, the reader is referred to the web version of this article.)

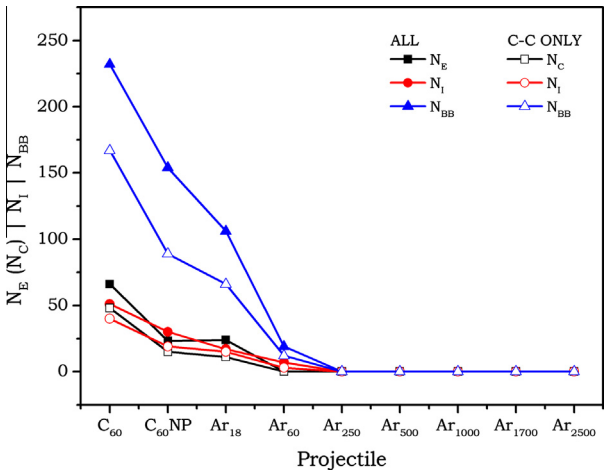

Fig. 3. The projectile dependent distributions of number of broken bonds (N_{BB}), newly created internal bonds (N_I) and newly created external bonds (N_E) calculated for all (C–C, H–H and C–H) bonds (solid points) and for C–C bonds only (open points) at 3 ps after bombardment. The C_{60} NP signature represents the analysis of the C_{60} bombardment in which bonds created by projectile atoms are not taken into account. (For interpretation of the references to colour in this figure legend, the reader is referred to the web version of this article.)

crease of kinetic energy per atom resulting from the increase of the number of atoms in the projectile as well as the increase of its lateral size. However, since only one initial kinetic energy is used in our calculation it is difficult to distinguish which of these parameters plays the dominant role. Additionally, due to the concomitant reduction of the velocity, the crater formation process is also much slower than in the case of C_{60} and small argon clusters.

The time evolution of bond-breaking during 2.5 keV C_{60}, Ar_{18} and Ar_{60} cluster bombardment is shown in Fig. 2. The plot marked as C_{60} NP represents the time evolution of bond-breaking during C_{60} bombardment, in which the number of C–C bonds broken in the projectile is subtracted from the total number of broken bonds. The general trend visible for all the shown projectiles is that, initially, there is a fast increase of the number of broken bonds while after ~400 fs all the curves start to saturate. They reach their constant value at the end of the simulation time in the case of Ar clusters and are close to full saturation in the case of C_{60} bombardment. For all of these clusters, 90–100% of broken bonds recorded after 3 ps of simulation time were broken within the first 500 fs. This corresponds to 97–99% of the total kinetic energy transferred from the projectile to the bombarded surface. The analysis of the kinetic energy distributions of atoms (Fig. 1) reveals that further bond-breaking is improbable because of the low energy of the atoms, for all the considered projectiles. The time evolution of the new internal and external bonds, as well as the time evolution of bond-breaking and the creation of new internal and external bonds for the case in which only C–C bonds are taken into account, are similar to the case of the time evolution of bond-breaking, with the only difference that the final values are lower (not shown).

The projectile dependent distributions of number of broken bonds (N_{BB}), number of newly created internal bonds (N_I) and number of newly created external bonds (N_E) calculated at 3 ps after the projectile impact are shown in Fig. 3. With the same total kinetic energy, C_{60} is able to break over two times more H–H, H–C and C–C bonds than Ar_{18} (which has a similar total mass), and over 12-times more bonds when compared to Ar_{60}, which has the same number of atoms (see Table 1 for more detailed values). However, the C_{60} projectile is made of carbon and has initially 90 C–C bonds which can be broken during collision with the surface of polystyrene. If the bonds broken within the projectile are not taken into account, the total number of broken bonds is reduced from the value of 232 to 154, i.e. ~87% of the C_{60} projectile bonds are broken during the impact. If one omits these internal bonds, the behavior of C_{60} is similar to Ar_{18}, in terms of final values of newly created external bonds/crosslinks and internal bonds. When the number of atoms in the Ar cluster increases, the total number of broken bonds (and newly formed bonds) decreases significantly and reaches the zero value for Ar_{250} and larger clusters.

There are several possible reasons for the fast reduction of the number of broken bonds observed with Ar cluster projectiles. Increasing the number of atoms in the projectile leads to the reduction of the kinetic energy per atom, to the increase of the total mass of the projectile and to the reduction of its velocity at the same time. As was shown by Delcorte et al. for the case of polyethylene bombardment [19] and Postawa et al. for the benzene [20], the transition from the Ar_{18} to larger Ar projectiles corresponds to the transition between region having high fragmentation rate to the region in which virtually no fragments are sputtered. The threshold energy per nucleon of this transition was calculated at ~1 eV/nucleon [19], which is close to the energy per nucleon for the Ar_{60} projectile used in our simulations. According to these studies, one cannot consider the interaction of large Ar clusters with the bombarded material simply as atom–atom collisions and expect bonds to be broken even if the initial energy per atom of the cluster (for instance, Ar_{250}) is higher than the energy of C–H and C–C bonds in the PS4 molecule. The interaction of large Ar clusters with the aPS4 should be analyzed in a more complex manner, as the collective effect of many atomic interactions. As shown in Fig. 1, larger Ar clusters interact with the sample in a relatively soft manner, by pushing PS4 molecules downward and sideways in a correlated motion. This should substantially reduce the efficiency of energy transfer between single projectile and target atoms. Additionally, the increase of the size of these projectiles causes that the energy of the projectile is provided in a much larger volume of the bombarded sample. However, to fully determine which parameter change has the greatest influence on the number of bonds, which are broken during Ar cluster bombardment, additional calculations for different initial kinetic energies of projectiles have to be performed.

The process of disintegration of bonds is not the only chemical process initiated in the organic material during bombardment by energetic clusters. As was explained in the "Model" section, after the bond scission, any two atoms which were initially connected

Table 1
The total number of broken bonds (N_B), newly created internal (N_I), newly created external bonds (N_E) and total number of molecule equivalents (N_{MOL}) taking part in chemical reactions occurring in the system calculated from the bombardment of amorphous polystyrene sample by C_{60}, Ar_{18} and Ar_{60} cluster projectiles with the initial kinetic energy of 2.5 keV. The last two columns represents the values of crosslinks (N_C) and N_C^{C60}/N_C^{PS4} ratio calculated from 2.5 keV bombardment of fullerite crystal [21].

Proj.	N_{BB}			N_I			N_E			N_{MOL}	N_C (C_{60})	N_C^{C60}/N_C^{PS4}
	ALL	C–C	Ratio	ALL	C–C	Ratio	ALL	C–C	Ratio			
C_{60}	232	167	0.72	51	40	0.78	66	48	0.73	19	152	3.8
C_{60} NP	154	89	0.58	30	19	0.63	23	15	0.65	19	77	5.1
Ar_{18}	106	66	0.62	17	15	0.88	24	11	0.46	19	82	7.5
Ar_{60}	19	12	0.63	7	3	0.43	0	0	–	4	12	–

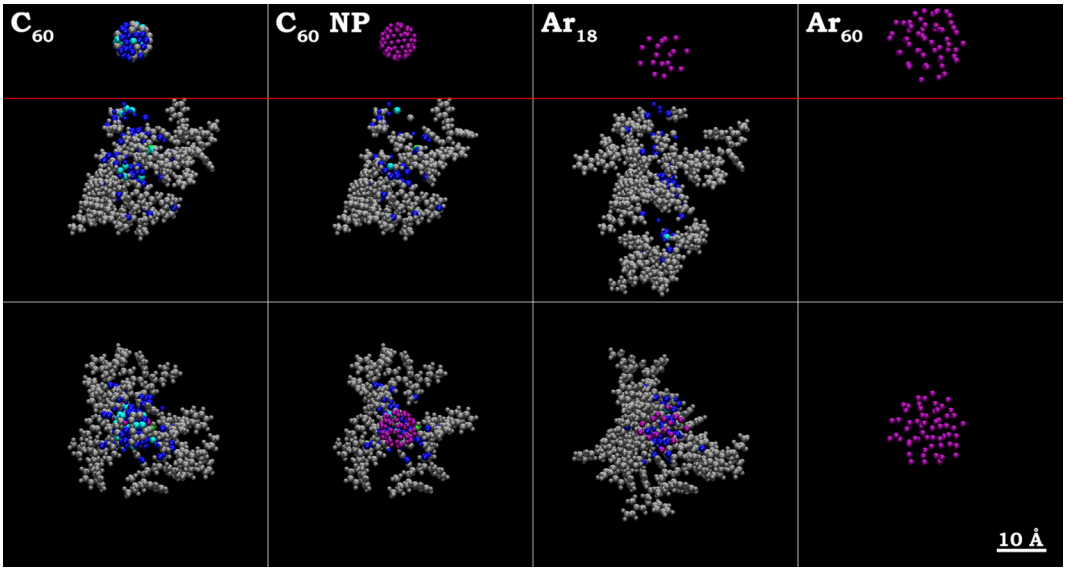

Fig. 4. Side (top) and top (bottom) view of the initial positions of particles containing atoms which create new external bonds. The color coding represents the number of external bonds for each atom as follows: gray – 0, blue – 1, cyan – 2, green – 3 and yellow – 4. Red line indicates the highest position of the polystyrene surface. (For interpretation of the references to color in this figure legend, the reader is referred to the web version of this article.)

by the broken bond may either (i) reconnect, (ii) remain disconnected, (iii) create a new internal bond with another atom belonging to the same molecule or (iv) create a new external bond with an atom belonging to a different molecule. The projectile dependent distributions of total numbers of newly created external and internal bonds are shown in Fig. 3. Both of these quantities follow the same trend as for the bond-breaking with the difference that the corresponding values are lower (Table 1). A more detailed analysis reveals that bonds formed by atoms of the C_{60} projectile constitute ~65 and ~41% of the newly formed external and internal bonds, respectively. When these bonds are not taken into account (the C_{60} NP case), the calculated values become comparable to those obtained for the Ar_{18} cluster bombardment. The only visible difference is the fact that Ar_{18} leads to creation of a larger number of external than internal bonds in the sample, while C_{60} shows the opposite trend. When Ar_{60} is used for bombardment, no new external and only few internal bonds are observed. As explained in the "Model" section, to obtain a realistic description of cross-linking, only new external C–C bonds should be considered (open points in Fig. 3). The data show that, depending on the projectile used, C–C bonds constitute up to ~72% of all the broken bonds. Eighty eight and 73% of the newly created internal (N_I) and external bonds (considered as crosslinks - N_C), respectively (Table 1), are also C–C bonds. Second, when the values of N_C and N_I calculated for C_{60} NP and Ar_{18} are compared, both projectiles induce the creation of a larger number of new internal bonds than crosslinks, which was not the case when all bond types were taken into account. Our results imply that, in general, C_{60} and Ar_{18} interact with polystyrene in a similar manner, and that the relatively larger number of crosslinks observed with C_{60} results from the chemical composition of the projectile.

Since our simulations end up at 3 ps we do not have the full picture of the sputtering process. In our case the total numbers of polystyrene molecule equivalents taking part in all the chemical reactions observed in the aPS4 sample are 19, 19 and 4 for C_{60}, Ar_{18} and Ar_{60} projectiles, respectively. However, we do not have any information about the efficiency of the sputtering process by different projectiles, which cannot be obtained in such a short time. As shown by Kennedy and Garrison for benzene [18] this efficiency is highest for the Ar_{60} projectile and the area of particle ejection is located in the closest neighborhood of the impact point. Fig. 4 shows the original positions of all the atoms belonging to the molecules containing newly created external bonds in the sample. The comparison between C_{60} and Ar_{18} projectiles reveals that the measured surface area occupied by of those particles is slightly larger for Ar_{18}. This is probably the consequence of the difference in the size of the projectiles, whose maximum radius is ~5.44 and 3.55 Å for Ar_{18} and C_{60}, respectively. However, if we consider only the newly bonded atoms we can see that their initial positions are located along the vertical track of the projectile for both clusters. This particular volume is the region of the strongest interaction of the projectile with the bombarded material. Additionally,

the maximum depth at which externally bonded atoms can be found is slightly larger for Ar_{18}, which can be related to the higher atomic mass and kinetic energy per atom of that cluster. The atomic mass mismatch leads to lower energy transfer efficiency than in the case of C_{60} and, hence, with the higher kinetic energy per atom, argon atoms are expected to penetrate deeper into the polystyrene sample. Similar trends are observed for the initial positions of atoms which create new internal bonds (not shown). The only difference is that the total volume occupied by the molecules and fragments containing these atoms is significantly smaller than for molecules and fragments containing externally bonded atoms. Assuming high efficiency of the material removal, one could expect that most of chemically interacting material should be removed. Experimentally, depth profiles are obtained in dynamic SIMS, in which overlapping of single sputtering cascades can occur, so that the final effect will be the interplay between the accumulation of intermolecular bonding in the sample and the material removal efficiency of the used projectile.

Finally, the comparison to the number of crosslinks calculated for the 2.5 keV Ar_{18} bombardment of a C_{60} fullerite crystal [21] indicates that the crosslinking process is almost 7.5-fold less efficient with the aPS4 sample than with the fullerite, when only C–C bonds are taken into account (Table 1). This in good agreement with the results published by Webb et al. proving that the presence of hydrogen in the organic material results in a significant reduction of the number of crosslinks [22].

4. Conclusion

The theoretical analysis of the bombardment of amorphous polystyrene surfaces by C_{60} and Ar clusters reveals that the relatively higher efficiency of the crosslinking process observed with C_{60} is directly related to the chemical composition of this projectile. C_{60} clusters deliver many highly reactive carbon radicals, having a significant impact on the number of crosslinks formed during bombardment. For this reason, Ar cluster projectiles should be better candidates for organic material depth profiling experiments, where crosslinking is the major problem. However, since our simulations are stopped at 3 ps after the impact we are unable to see how many of the crosslinking molecules will remain in the solid, so the final crosslinking effect will depend also on the sputtering efficiency of the used projectiles. Another important observation concerns the reduction of the crosslinking with increasing Ar cluster size, which indicates that large clusters should also be preferred to small clusters ($<\sim 10^2$ atoms) for those experiments. In order to derive more general rules and to better identify the physical parameters (projectile nuclearity, size, energy per atom) underlying the cluster-induced crosslinking process, a molecular dynamics study of the effect of the projectile energy is underway.

Acknowledgments

B.C. and A.D. wish to thank the Belgian Fonds National pour la Recherche Scientifique (FNRS) for financial support. B.J.G. acknowledges financial support from Grant CHE-0901564, which is administered by the Chemistry Division of the National Science Foundation. Computational resources were provided by the Institut de calcul intensif et de stockage de masse at Université Catholique de Louvain.

References

[1] N. Winograd, Anal. Chem. 77 (2005) 142A.
[2] C.M. Mahoney, Mass Spectrom. Rev. 29 (2010) 247.
[3] Z. Takats, J.M. Wiseman, B. Gologan, R.G. Cooks, Science 306 (2004) 471.
[4] M.A. Meetani, Y.S. Shin, S. Zhang, R. Mayer, F. Basile, J. Mass Spectrom. 42 (2007) 1186.
[5] J. Laskin, B.S. Heath, P.J. Roach, L. Cazares, O.J. Semmes, Anal. Chem. 84 (2012) 141.
[6] C.C. Chan, M.S. Bolgar, S.A. Miller, A.B. Attygalle, J. Am. Soc. Mass Spectrom. 21 (2010) 1554.
[7] C.C. Chan, M.S. Bolgar, S.A. Miller, A.B. Attygalle, J. Am. Soc. Mass Spectrom. 22 (2011) 173.
[8] I. Yamada, J. Matsuo, N. Toyoda, T. Aoki, E. Jones, Z. Insepov, Mat. Sci. Eng. A 253 (1998) 249.
[9] S. Ninomiya, Y. Nakata, K. Ichiki, T. Seki, T. Aoki, J. Matsuo, Nucl. Instr. Meth. Phys. Res. B 256 (2007) 493.
[10] T. Mouhib, C. Poleunis, R. Mollers, E. Niehuis, P. Defrance, P. Bertrand, A. Delcorte, Surf. Interface Anal. (2012), http://dx.doi.org/10.1002/sia.5052.
[11] B.J. Garrison, in: J.C. Vickerman, D. Briggs (Eds.), TOF-SIMS Surface Analysis by Mass Spectrometry, Surface Spectra, Manchester, U.K., 2001, p. 223.
[12] W.D. Wilson, L.G. Haggmark, J.P. Biersack, Phys. Rev. B 15 (1977) 2458.
[13] M.P. Allen, D.J. Tildesley, Computer Simulation of Liquids, Clarendon Press, Oxford, U.K., 1987. p. 7.
[14] S.J. Stuart, A.B. Tutein, J.A. Harrison, J. Chem. Phys. 112 (2000) 6472.
[15] D.W. Brenner, Phys. Rev. B 42 (1990) 9458.
[16] A. Delcorte, B.J. Garrison, J. Phys. Chem. B 108 (2004) 15652.
[17] B.J. Garrison, Z. Postawa, Mass Spectrom. Rev. 27 (2008) 289.
[18] P.E. Kennedy, B.J. Garrison, Surf. Interface Anal. (2012), http://dx.doi.org/10.1002/sia.5022.
[19] A. Delcorte, B.J. Garrison, K. Hamraoui, Anal. Chem. 81 (2009) 6676.
[20] Z. Postawa, R. Paruch, L. Rzeznik, B.J. Garrison, Surf. Interface Anal. (2012), http://dx.doi.org/10.1002/sia.4927.
[21] A. Delcorte, O.A. Restrepo, B. Czerwinski, B.J. Garrison, Surf. Interface Anal. (2012), http://dx.doi.org/10.1002/sia.4926.
[22] R.P. Webb, B.J. Garrison, J.C. Vickerman, Surf. Interface Anal. 43 (2011) 116.